Size Selective and Volume Exclusion Effects on Ion Transfer at the Silicalite Modified Liquid−Liquid Interface

Michael J. Stephenson,[†] Andrew J. King,[†] Stuart M. Holmes,[‡] and Robert A. W. Dryfe*[,†]

School of Chemistry and School of Chemical Engineering and Analytical Science, University of Manchester, P.O. Box 88, Manchester, United Kingdom M60 1QD

Received: April 6, 2005; In Final Form: August 5, 2005

The modification of the liquid/liquid interface with membranes of silicalite, a neutral framework zeolite, is used to extend the potential window. This feature allows the observation of the transfer of extremely hydrophilic ions, due to the size-exclusion of organic ions from the interior of the zeolitic framework. Similarly, volume exclusion effects are shown to affect facilitated ion transfer processes involving alkali metal cations. In contrast, proton transfer is largely unaffected by the presence of the zeolite, which is suggestive of more rapid diffusion processes within the interior of the framework. The technique of liquid/liquid electrochemistry should allow the measurement of solution phase transport parameters for ions within microporous hosts.

Introduction

Size selective transport properties are highly important in a number of areas including catalysis,[1,2] separation,[3] and chemical sensing.[4,5] Interest in this area has led to numerous studies of size selectivity and transport properties of porous crystalline materials, particularly for zeolites and related materials. Despite this interest, the bulk of the available data relates to gaseous diffusion processes: there is a need for further experimental study of solution phase transport measurements within zeolites, particularly for ionic species. Zeolites' size selective properties arise from the exclusion of species with diameters larger than the pores or channels. A related property is volume exclusion, which arises where the pore size is large enough to allow species to diffuse through unhindered, but the pore volume is limited, and so the zeolite has a limited storage capacity. This is especially important for zeolites with a charged framework and large counterions.[6] The size selective properties of zeolites have been exploited for shape selective catalysts, where the zeolite channel geometry restricts the transport of reactants and controls the size and shape of transition states and products.[1,2]

Electrochemical methods have been employed to determine fluxes through materials that exhibit size, or charge, based selectivity.[7] Zeolites have been used to modify electrode surfaces and so imbue them with specific properties such as enhancement of electrocatalytic behavior,[8] or to act as templates for metal deposition.[9] An important goal in combining microporous materials with electrochemistry is the study of size and/or charge based molecular sieving, imparted by the zeolite. Size selective electrochemical responses have been achieved by preparing thin films of tetrarhenium square assemblies supported on gold or glassy carbon electrodes: these systems also have the additional benefit in that the channel sizes are adjustable by synthetic variations.[10] Polymeric membranes containing a collection of monodispersed gold nanotubules have been used to separate species with diameters of less than 1 nm from larger species.[11] Earlier work on the zeolite modification of electrified interfaces generally used zeolite containing composites, because of difficulties in preparing continuous zeolite structures:[12,13] this made it difficult to observe truly size selective properties. We have pursued an alternative approach, using zeolites to modify electrified liquid/liquid interfaces, to imbue size selective properties. This has been demonstrated previously,[14,15] where the modification of the interface with a silicalite membrane selectively blocked tetraethylammonium cation (TEA) transfer, but allowed tetramethylammonium cation (TMA) transfer. Ions can be driven to the adjacent immiscible liquid phase by the application of a potential difference across the liquid/liquid interface.[16,17] Typically an interface between an aqueous phase and solvents such as nitrobenzene or 1,2-dichloroethane (DCE) is employed. The transfer of hydrophilic ions can be facilitated by the use of a complexing agent in the organic phase (e.g., crown ethers), this stabilizes the transferred ion, and in doing so, lowers the required transfer potential. Ion-selective sensing has been reported,[18,19] along with a recent report on the electrochemically enhanced ion-exchange of zeolites.[20] In all of these cases selectivity is important and the potential of ion transfer can be used either to identify or to transfer specific ions. An alternative approach to ion sensing at the liquid/liquid interface uses a hydrophobic membrane to separate two aqueous solutions.[21] This configuration also extends the observable potential window, allowing the transfer of hydrophilic ions to be observed.

The intracrystalline diffusion of sorbates in zeolites can have a dramatic effect on catalyst performance, and a better understanding of diffusion could lead to further optimization of existing commercial applications and the development of new applications.[22] There are a number of techniques available for measuring intracrystalline diffusion, including quasielastic neutron scattering,[23] pulse field gradient nuclear magnetic resonance,[24] chromatographic methods such as the zero length column method (ZLC),[25] and catalytic measurements.[26] These methods have found that intracrystalline diffusion is dependent on the size of the pores, the size, shape, and concentration of the sorbate, the Al/Si ratio of the framework, and the temperature. The majority of these studies relate to vapor phase

* Address correspondence to this author. E-mail: robert.dryfe@manchester.ac.uk. Fax: +44 (0)161-306-4559.

[†] School of Chemistry.

[‡] School of Chemical Engineering and Analytical Science.

10.1021/jp051774a CCC: $30.25
Published on Web 09/22/2005

systems, although many industrial processes are carried out under liquid-phase conditions. Techniques employed to investigate liquid-phase systems include liquid chromatography[27] and the liquid-phase ZLC method.[28] The intra-zeolitic diffusion of ions has received even less attention, one such paper utilizes chronoamperometry to investigate silver ion diffusion in zeolite Y.[29] The interior of zeolites represents an unusual diffusion regime, where deviations from purely Fickian behavior may be observed.[30] Electrochemical methods could, conceivably, offer an alternative route to probe intra-zeolite transport. Data analysis is complicated, however, because of difficulties in meeting the experimental conditions usually required in electrochemical experiments (e.g., excess supporting electrolyte over analyte, to eliminate migration and minimize solution phase resistance).

The aim of this paper is to determine the effect modification of the liquid/liquid interface with a silicalite membrane has on ion transfer, specifically relating changes in ion transfer to size selective and volume exclusion properties of the silicalite membrane. As well as altering ion transfer, it is proposed that this technique can provide insight into the diffusion of ions within the silicalite membrane. Silicalite was the zeolite of choice as it has an uncharged framework, so there are no complications with associated counterions. Silicalite has a three-dimensional structure constructed from corner sharing SiO_4 tetrahedra. These form a regular structure with uniform pore and cavity size. Silicalite consists of both straight and sinusoidal 10(Si) atom ring channels with diameters of 5.6 × 5.3 and 5.5 × 5.1 Å, respectively, and has internal cavity diameters of about 9 Å.[31]

Experimental Section

Chemicals. Silicalite membranes were synthesized according to the method described by Kiyozumi et al.,[32] in the presence of an organic template, tetrapropylammonium bromide. The free-standing membrane was prepared on a mercury surface, and subsequently calcined in air at 450 °C to remove the template. The membranes employed in this study had a typical thickness of about 0.5 mm. All aqueous solutions were made with water obtained from an "ELGA purelab ultra" purification system (Vivendi Water Systems Ltd., High Wycombe, UK) and all organic solutions were made with DCE (99.8%+, Aldrich, Dorset, UK) as the solvent. NaCl (99+%, Aldrich), LiCl (99+%, Aldrich), KCl (99+%, Aldrich), tetramethylammonium chloride (TMA Cl, 99+%, Fluka, Dorset, UK), tetraethylammonium chloride (TEA Cl, 99+%, Fluka, Dorset, UK), magnesium sulfate (puriss, Fluka), and sulfuric acid (ARISTAR grade, BDH Laboratory Supplies, Poole, UK) were used as aqueous electrolytes. Dibenzo-18-crown-6 (DB18c6, 98%, Lancaster Chemicals Co., Morecambe, UK) was employed as the complexing agent and was dissolved in the organic phase. Bis(triphenylphosphoranylidene)ammonium tetraphenyl borate (BTPPATPB), bis(triphenylphosphoranylidene)ammonium tetrakis(4-chlorophenyl) borate ($BTPPATPBCl_4$), and bis(triphenylphosphoranylidene)ammonium tetrakis(pentafluorophenyl) borate ($BTPPATPBF_{20}$) were used as organic background electrolytes. These salts were prepared by metathesis of bis(triphenylphosphoranylidene) ammonium chloride (99%+, Aldrich) and sodium tetraphenylborate (Aldrich), potassium tetrakis(4-chlorophenyl)borate (Fluka), or lithium tetrakis(pentafluorophenyl) borate (Boulder Chemical Co., Boulder, CO), respectively, according to a previously reported procedure.[33]

Electrochemical Cells. Silicalite membranes of ca. 9 mm diameter were attached to a glass tube with silicone rubber compound (RS components, Corby, UK). The electrochemical cell design was similar to the arrangement previously reported for voltammetry at the zeolite-modified liquid/liquid interface.[14,15] The silicalite membrane was generally left in contact with the aqueous solution overnight, before being immersed in the organic phase for voltammetric experimentation. The purpose of the membrane saturation process was to allow the aqueous phase to penetrate the internal volume of the zeolite (vide infra). Equivalent experiments were also performed at the "bare" water/DCE interface. A silver/silver chloride or silver/silver sulfate reference electrode was used in the aqueous phase and a silver/silver tetraphenylborate pseudo-reference electrode was used in the organic phase, prepared according to a method previously described.[34] Platinum gauze was used as the counter electrode in both phases. The water/DCE interface was polarized by using a four-electrode potentiostat (Autolab PGSTAT 100, Eco-chemie, Utrecht, Netherlands). Positive feedback compensation was applied, via the potentiostat, to counter-act the ohmic drop within the cell. The cell resistance was typically on the order of 2000 Ω, although this increased substantially if the presaturation with the aqueous phase was not performed. All experiments were performed at room temperature (293 ±3 K). The electrochemical cells can be written as:

Cell 1: $Ag_{(S)}|AgTPB_{(S)}|0.02\ M\ BTPPATPB_{(DCE)}||0.02\ M\ MgSO_{4(aq)}|Ag_2SO_{4(S)}|Ag_{(S)}$

Cell 2: $Ag_{(S)}|AgTPB_{(S)}|0.02\ M\ BTPPATPBCl_{4(DCE)}||0.05\ M\ TMACl_{(aq)}|AgCl_{(S)}|Ag_{(S)}$

Cell 3: $Ag_{(S)}|AgTPB_{(S)}|0.02\ M\ BTPPATPBCl_{4(DCE)}||1\ mM\ TEACl_{(aq)} + 0.1\ M\ LiCl_{(aq)}|AgCl_{(S)}|Ag_{(S)}$

Cell 4: $Ag_{(S)}|AgTPB_{(S)}|0.02\ M\ BTPPATPBCl_4,\ 1\ mM\ DB18c6_{(DCE)}||0.1\ M\ YCl_{(aq)}|AgCl_{(S)}|Ag_{(S)}$

Cell 5: $Ag_{(S)}|AgTPB_{(S)}|0.02\ M\ BTPPATPBF_{20},\ 1\ mM\ DB18c6_{(DCE)}||0.01\ M\ H_2SO_{4(aq)}|Ag_2SO_{4(S)}|Ag_{(S)}$

The double bar denotes the polarized interface. For cell 4, YCl was LiCl, NaCl, or KCl. Cells 1−5 can be subdivided into two classes, (a) where the bare water/DCE interface is used and (b) where the silicalite membrane is present at the water/DCE interface.

Results and Discussion

Simple Ion Transfer. The potential window available for voltammetry at the liquid/liquid interface is defined by the standard transfer potentials of the supporting electrolyte ions within each phase.[35] The voltammetric response of the liquid/liquid interface is consequently characterized by positive and negative potential limits, which are associated with the transfer of ions from the background electrolytes across the interface. The cyclic voltammograms in Figure 1 show the potential window in the absence and presence of a silicalite membrane at the liquid/liquid interface. As can be clearly seen, the presence of the silicalite membrane significantly increases the potential window. This extension occurs because the diameter of the silicalite pores (see Introduction) excludes the transfer of the larger TPB anion (van der Waals diameter of 8.4 Å),[36] but allows the transfer of the smaller Mg^{2+} cation (crystallographic diameter of 1.72Å).[37] The observed increase in the positive limit of the potential window proves that the hydrophilicity of Mg^{2+} exceeds the lipophilicity of TPB^-. In this way it is possible to

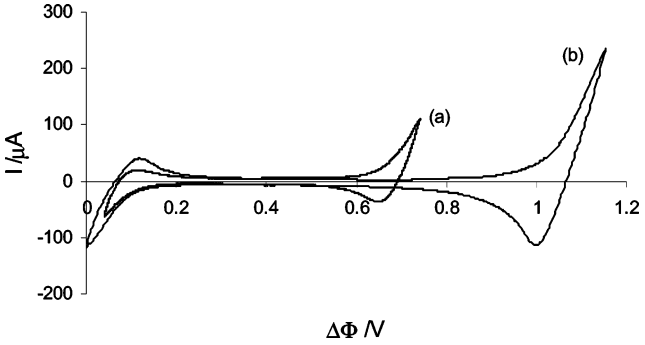

Figure 1. The cyclic voltammetric data for the blank potential window in the absence (a) and presence (b) of a silicalite membrane, using cell 1 with a voltage scan rate of 0.1 V s^{-1}.

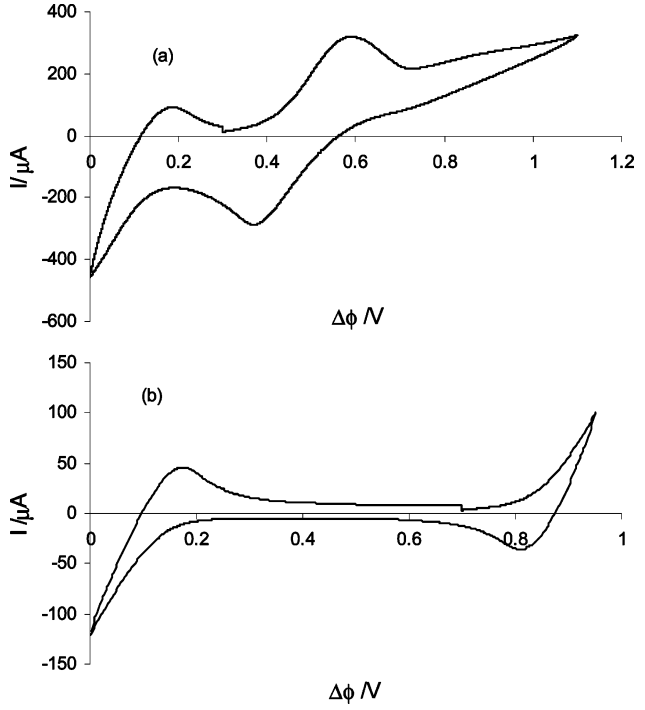

Figure 2. The cyclic voltammetric data for (a) cell 2 and (b) cell 3, in the presence of a silicalite membrane at the liquid/liquid interface, with a voltage scan rate of 0.1 V s^{-1}.

measure the potential of ion transfer of very hydrophilic ions, in this case Mg^{2+}, which would normally transfer beyond the potential window. The difference in observed half-wave potentials between TPB^- and Mg^{2+}, Δ ($\Delta\phi^{1/2}$) = 0.356 V, can be combined with the literature value for TPB^- transfer ($\Delta\phi^{1/2}$ = 0.342 V on the tetraphenylarsonium tetraphenylborate scale).[38] The experimental half-wave potentials were determined, even though only the foot of the voltammetric wave was observed in each case, using the method developed by Shao et al.[38] Adjusting the values to the tetraphenylarsonium tetraphenylborate scale gives a $\Delta\phi^{1/2}$ value for Mg^{2+} of 0.698 V.

To confirm the size selective properties of the silicalite-modified interface, the transfer of TMA^+ (van der Waals diameter of 5.2 Å)[39] and TEA^+ (van der Waals diameter of 6.2 Å)[39] was investigated. The cyclic voltammograms in Figure 2a clearly show that TMA^+ is able to transfer, whereas TEA^+ is unable to transfer in the presence of a silicalite modified interface (see Figure 2b). This sieving effect is consistent with the ionic sizes relative to those of the silicalite pores, where TEA^+ should be excluded from entering the silicalite membrane and crossing the interface. An interesting feature to note is that TMA^+ Cl^- was the sole electrolyte in the aqueous phase, and after the TMA^+ transfer peak there was no apparent positive limit to the potential window. We attribute the general increase in current beyond 0.7 V to the transfer of TMA^+ ions from the second layer of crystallites within the membrane (see below). There is, however, a point of inflection at ca. 0.9 V, which is the approximate potential of transfer of $TPBCl_4^-$.[38] The inflection point indicates that the transfer of residual TMA^+ ions may be suppressed slightly by the presence of the size-excluded $TPBCl_4^-$ ions on the organic side of the membrane, which therefore occlude the exit of the TMA^+ ions. The voltammetric response attributed to the transfer of the TMA^+ from the first layer of crystallites is distorted, with a separation between the egress (transfer to organic) and ingress (return from organic) peaks of ca. 0.24 V, four times greater than the value expected for univalent ion transfer at room temperature under purely diffusive control. Much of this discrepancy arises because of the "nonclassical" conditions of the experiment: the concentration is relatively high, no other electrolyte is present hence migration will contribute to the ionic flux, and the inherent resistance of liquid/liquid electrochemical systems is amplified by the presence of the silicalite membrane. We note that models have been developed for such cases, where resistive distortions of voltammetry result.[40,41] Comparison of the data from these numerical models suggests that the peak potential (E_p) should depend on the peak current (I_p) to the power 0.929:[40] application of this model to the TMA^+ system of Figure 2 gave the plot shown in the Supporting Information (Figure S1). The gradient of the E_p vs $I_p^{0.929}$ plot can be used to determine the residual (i.e., uncompensated remainder) of resistance within the cell, as it is given at 298 K by[40]

$$\text{grad} = 1.036[(1 - \gamma)R^0]^{0.929} \quad (1)$$

where R^0 is the resistance between the reference electrode and the active interface, and γ is the proportion of this resistance that is compensated experimentally. This analysis gives a residual resistance value of 200 Ω. If we approximate R^0 to the cell resistance, the observed resistance value is consistent with the experimentally observed values (vide supra), on the basis that γ is ca. 0.9. Similarly, the dependence of I_p on the square root of voltage scan rate can be used to determine an apparent diffusion coefficient for TMA^+, although such an approach neglects the additional migratory flux and the distortion of the volammetry due to the residual cell resistance.

The silicalite membrane is made up of randomly orientated crystals, intergrown to form a coherent structure. The voltammetric data of Figures 1 and 2 indicate that the silicalite membrane is coherent, since otherwise significant "leakage" currents, due to the transfer of size-excluded ions across defects, would be observed.

Facilitated Ion Transfer (FIT). The cyclic voltammograms in Figure 3 show the FIT of (a) K^+, (b) Na^+, (c) Li^+, and (d) H^+ assisted by DB18c6, in the absence and presence of a silicalite membrane at the liquid/liquid interface. The two sets of results are very similar, although three distinguishing factors can be identified. First, in the case of sulfuric acid as the aqueous electrolyte, the negative potential limit is extended by ca. 0.055 V in the presence of the silicalite membrane (if it is assumed that FIT of H^+ occurs at the same potential in the presence and absence of silicalite). Second, by contrast, the potential window with LiCl as the aqueous electrolyte has a less positive limit in the presence of silicalite than in the absence of silicalite. A third distinction is that in the presence of silicalite K^+, Na^+, and Li^+ facilitated ion transfer currents tend toward a plateau, whereas for H^+ and the unmodified interfaces a typical peak current

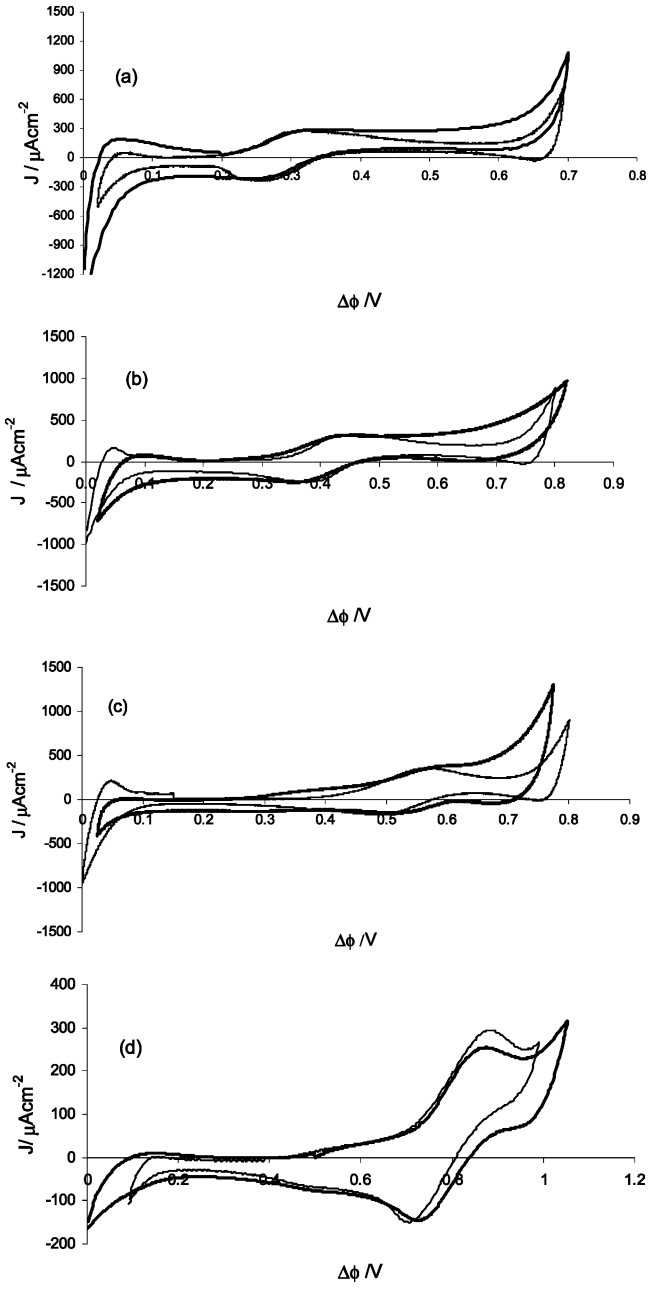

Figure 3. The cyclic voltammetric data for (a) K^+, (b) Na^+, (c) Li^+, and (d) H^+ in the presence (thick line) and absence (thin line) of a silicalite membrane using cells 4 and 5 with a voltage scan rate of 0.1 V s^{-1}. Current densities, *J*, were calculated from the active area of the interface, 1.13 and 0.38 cm^2 for the "bare" and silicalite modified interfaces, respectively.

profile (indicative of linear diffusion) is produced. The increase in the negative potential limit in the presence of silicalite when using sulfuric acid as the aqueous electrolyte indicates, that in the case of the unmodified interface, the window is limited by the transfer of BTPPA cations from the organic to aqueous phase. For an intact silicalite modified interface, $BTPPA^+$ (crystallographic diameter of 11.0×7.4 $Å^2$)[42] is size excluded from transferring. Instead the sulfate anion (diameter of 5.1 Å)[43] transfer from the aqueous to organic phase defines the negative potential limit. If we assume that the facilitated transfer of protons occurs at the same potential in the presence and absence of silicalite, then the observed difference in half-wave potentials of $BTPPA^+$ and SO_4^{2-} (0.010 V) can be used to determine the transfer potential of the organic cation. The half-wave potentials were again calculated, from the lower part of the observed

TABLE 1: Bare and Hydrated Ion Diameters of the Electrolyte Ions

ion	bare ion diameter/nm	hydrated ion diameter/nm	ref
K^+	0.30	0.44	42
Na^+	0.23	0.61	42
Li^+	0.14	0.70	42
H^+	0.037		35
Mg^{2+}	0.17	>0.9*	35
TEA^+	0.67	not hydrated	37
TMA^+	0.56	not hydrated	37
$BTPPA^+$	1.10×0.74	not hydrated	38
TPB^-	0.84	not hydrated	34
Cl^-	0.33	0.64	42
SO_4^{2-}	0.51		39

voltammetric waves, using the method described by Shao et al.,[38] yielding values of 0.110 and 0.100 V respectively for $BTPPA^+$ and SO_4^{2-} transfer on the arbitrary potential scale of the experiment. There is little accurate transfer equilibrium data on these ions at the water/DCE interface, although a recent report gives an approximate $\Delta\phi^{1/2}$ value of -0.88 V for sulfate at this interface.[44]

It has been reported that hydrophilic ions transfer from water to nitrobenzene with their hydration shells intact.[45] Table 1 shows the diameters of some hydrated ions. In the case of lithium ions the hydrated ion is larger than the pore size, so the observation of lithium transfer at the silicalite-modified interface implies that either this ion is stripped of some of its hydration shell, or the shell is distorted and loses its predicted spherical geometry. So far we have assumed that the standard potential of ion transfer, $\Delta_o^w \phi_i^0$, is the same in the presence and absence of silicalite. This may be inaccurate as the standard potential of ion transfer is related to Gibbs energy of transfer, $\Delta G_{tr,i}^{0,w\rightarrow o}$, (see eq 2), which is the difference in molar Gibbs energy of

$$\Delta_o^w \phi_i^0 = \frac{\Delta G_{tr,i}^{0,w\rightarrow o}}{z_i F} \tag{2}$$

solvation in the organic phase, $\mu_i^{0,o}$, and Gibbs energy of hydration, $\mu_i^{0,w}$ (see eq 3) where *i* is the ion transferred, z_i is the

$$\Delta G_{tr,i}^{0,w\rightarrow o} = \mu_i^{0,o} - \mu_i^{0,w} \tag{3}$$

charge of ion *i*, and *F* is Faraday's constant.

One may expect that the Gibbs energy of hydration would differ within the silicalite pore network, due to stabilizing/destabilizing effects of the internal surface and the fact that the channel size may limit the hydrated ion size. The data collated in Table 1 suggest that Li^+ does not have a complete hydration shell within silicalite,[46] which would increase $\mu_{Li}^{0,w}$, and correspondingly decrease the Gibbs energy of transfer and, in turn, the potential of ion transfer (from eq 2). This would explain why the positive limit of the potential window, using LiCl as the aqueous electrolyte in the presence of silicalite, is less positive than that in the absence of silicalite. Here we have assumed that the FIT peak is not shifted in the presence of silicalite. This assumption stems from the observation that the FIT peaks are typically at the same position relative to the positive and negative potential limits of the voltammogram, with or without the zeolite (see Figure 3a−c). We note that the complexation mechanism in the absence of silicalite involves some stripping of the hydration shell of the ion, as the inner cavity of the ligand, DB18c6 (~2.8 Å),[47] is smaller than that of the hydrated lithium cation.

A peak current response is indicative of ion transfer limited by linear diffusion; this type of diffusion regime is typically found for macroscopic interfaces. A plateau current is indicative of a steady state response, typically where radial diffusion limits ion transfer. Liquid−liquid analogues of microelectrodes, such as microholes, give a steady-state voltammetric response,[48] which is due to the radial diffusion field. For the experiments performed here, the current maximum was found to be proportional to the square root of the scan rate, both in the absence and with the presence of silicalite, which indicates a linear diffusion regime. These Randles−Sevèik plots produced diffusion coefficients ($4.6 \pm 0.2 \times 10^{-6}$ cm^2 s^{-1} in the absence of silicalite, $3.8 \pm 0.3 \times 10^{-6}$ cm^2 s^{-1} in the presence of silicalite) similar to the literature value of DB18c6 in DCE (4.55×10^{-6} cm^2 s^{-1}).[49] This suggests that the nano-array of pores on the organic face behave as a continuous active surface, rather than a series of distinct diffusion fields, so the individual radial diffusion fields overlap to form a single linear diffusion field. This observation was supported by analysis of the geometry, in a previous paper,[15] of the silicalite membrane in terms of the model of partially blocked electrode surface.[50] Therefore the pseudo-steady state appearance of the cyclic voltammogram in the presence of silicalite is not due to a radial diffusion field. Another possible explanation for the voltammetric waveshape is that the concentration of the aqueous electrolyte is lower than expected because of volume exclusion effects within the silicalite membrane. Experiments were attempted with use of low concentrations of transferring ion and complexing agent for the unmodified L/L interface (data not shown), but no evidence of a steady-state response was observed. Figure 3d shows that proton transfer is unaffected by the presence of silicalite, which suggests that the steady state response may be due to the size and diffusivity of the ion within the silicalite membrane. We also note that the capacitance of the silicalite modified interface is considerably higher than that of the bare interface (see Figures 1 and 3). Since only the facilitated proton-transfer peak gave a distinct peak-shaped response, the experimental data of Figure 3d were compared against a numerical simulation (using an implicit finite-difference procedure)[51] of the ion transfer problem, assuming one-dimensional diffusion. The experimental voltammogram, as with the TMA^+ system, gives a peak separation considerably larger than the anticipated 0.06 V. The Supporting Information (Figure S2) shows the comparison of the facilitated proton transfer through silicalite (bold line) with the numerical simulation of the ideally reversible transfer (dashed line). The effects of uncompensated resistance on voltammetry are known to be very similar to those of finite charge-transfer kinetics,[52] hence a second simulation was performed with quasireversible kinetics to increase the peak separation to the value observed experimentally at this scan rate (solid line). The agreement between the latter two cases is good, although an unidentified pre-peak is noted in the experimental response, which indicates that distortions (attributed to uncompensated resistance, as seen with TMA^+) are present in the proton-transfer data. We note that the other facilitated transfer systems give peak separations in Figure 3a−c close to the ideal value at room temperature (0.06 to 0.07 V), despite the current densities being at least as large as those seen in the proton case.

An important aspect to consider in the analysis of these experiments is the position of the interface in the presence of a silicalite membrane. Prior to each experiment the silicalite membrane was soaked in the aqueous solution for a minimum of 24 h, to ensure that it was water saturated. The aqueous phase was therefore expected to fill the pores and form an array of

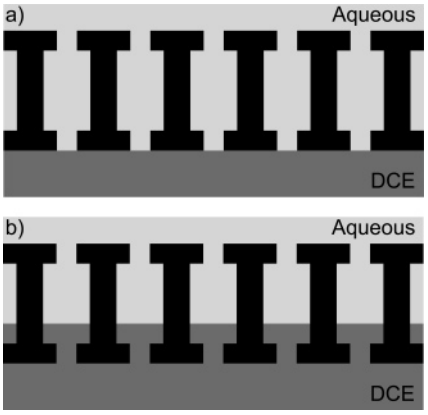

Figure 4. Schematic of the position of the liquid/liquid interface relative to the silicalite membrane: (a) at the mouth of the pores and (b) within the pore system.

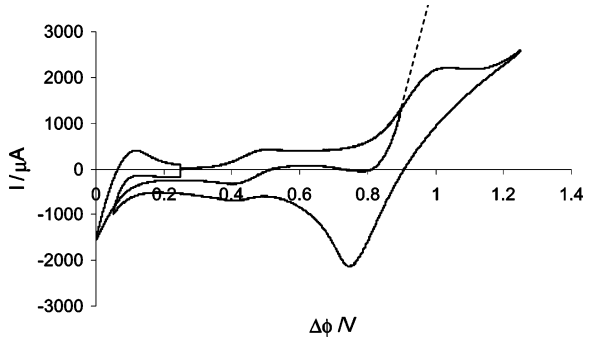

Figure 5. The cyclic voltammetric data for Na^+ in the presence of the silicalite membrane, two scans of same system: one within the conventional potential limits and the other examining the right-hand side of the potential window, using cell 4 with a voltage scan rate of 0.1 V s^{-1}.

interfaces with the organic phase, as per Figure 4a. If the interface were recessed within the silicalite pores, as per Figure 4b, then the FIT of the Group I ions would be inhibited, as the complexing agent is size excluded from entering the pores. Figure 3 suggests that the facilitated transfer of the Group I ions has not been inhibited, which in turn implies that the interface is located at the mouth of the pores. A more in-depth mechanistic investigation of FIT corroborates these results.[53] Another indication of the location of the interface is the resistivity of the cell; membranes that were soaked in the aqueous phase for longer were found to have lower resistivity. The lower resistivity can be accounted for because the organic electrolyte is size excluded from the pores, so as the interface penetrates the pores, there is an electrolyte depleted zone within the membrane. Overall these findings indicate that the interface is located at/near the mouth of the pores.

Extension of the Potential Window. The unassisted transfer of metal ions in the presence of the silicalite membrane was investigated by extending the positive potential limit, since this limit in the presence of silicalite is defined by the unassisted transfer of cations from the aqueous phase to the organic phase (see above). Figure 5 shows an example of a cyclic voltammogram for a silicalite modified interface. The FIT peak for Na^+ occurs at ca. 0.49 V and the unassisted transfer occurs at >0.8 V. The cyclic voltammogram from a "bare" interface would be expected to show a rapid current increase with small increases of potential at the positive limit (as per the dotted line) as there is normally a high concentration of the transferring ion. In the silicalite case, there is a much more gradual increase in current with increasing potential. Uncompensated resistance

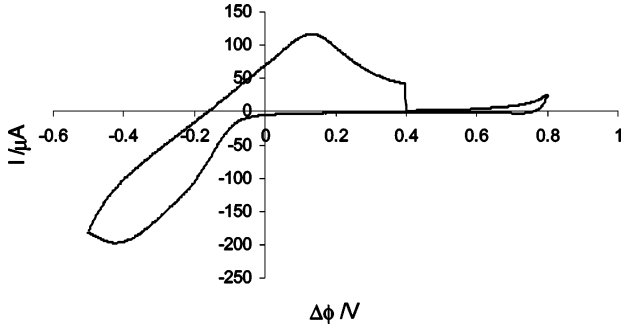

Figure 6. The cyclic voltammetric data for Li^+, examining the extended left-hand side of the potential window, using cell 4 with a voltage scan rate of 0.1 V s^{-1}.

effects could be responsible; however, we recall that the peak separation of the facilitated Na^+ peak is close to the ideal value. An alternative explanation is that the silicalite acts to reduce the effective interfacial concentration of aqueous electrolyte, relative to the bulk solution, by volume exclusion effects. The gradual increase in current implies that the aqueous electrolyte is slow to replenish at the interface. This may be due to diffusion of the ion within the silicalite pores being impeded, diffusion of ion across grain boundaries between silicalite crystallites being slow, and/or the existence of a kinetic barrier for the entry of ions to the silicalite membrane. It should be noted, however, that the thickness of the membrane is larger than the diffusion layer thickness established by the depletion of ions, on the experimental time scale. The maximum diffusion layer thickness, δ, can be calculated by[54]

$$\delta = \sqrt{2Dt} \tag{4}$$

where D is the diffusion coefficient and t is the time of the experiments. This equation applies for potential step experiments, and so will over-estimate the value compared to cyclic voltammetry experiments. In this case if the parameters from bulk solution are assumed to hold, D would be 1.3×10^{-5} cm^2 s^{-1} and t was ca. 10 s, hence δ was on the order of 0.02 cm, compared to a membrane thickness of 0.05 cm.

Another noticeable feature of Figure 5 is that an apparent pulse of sodium transfer occurs at ca. 1.0 V, which is superimposed on the gradual slope. This pulse is attributed to the transfer of ions already within the first layer of silicalite crystallites, whereas the underlying current is attributed to ions travelling between crystallites to the first layer and then across the interface. The pulse is significantly reduced after the first sweep. The system had to be left at equilibrium for at least 5 min before the pulse was fully recovered. This is consistent with the previous argument that ions within the first layer of silicalite crystallites are easy to remove, but replenishment is slow. Figure 6 shows that the same phenomenon is found on extension of the negative potential limits, but in this case the pulse of current is attributed to the transfer of chloride anions from the first layer of crystallites. As with the pulse of Figure 5, the high electrolyte concentration and lack of supporting electrolyte mean that the pulse is distorted compared to that expected for conventional voltammetry. Figure 7 shows that if the cell is taken to increasingly high potentials a second pulse can be observed. This second pulse was only seen for H^+ transfer: none of the other ions investigated produced a second peak. The occurrence of the second peak would be consistent with a more rapid intracrystalline diffusion process, so a second pulse is produced by the more rapid transfer of protons from the second layer of silicalite crystallites. It should be noted that

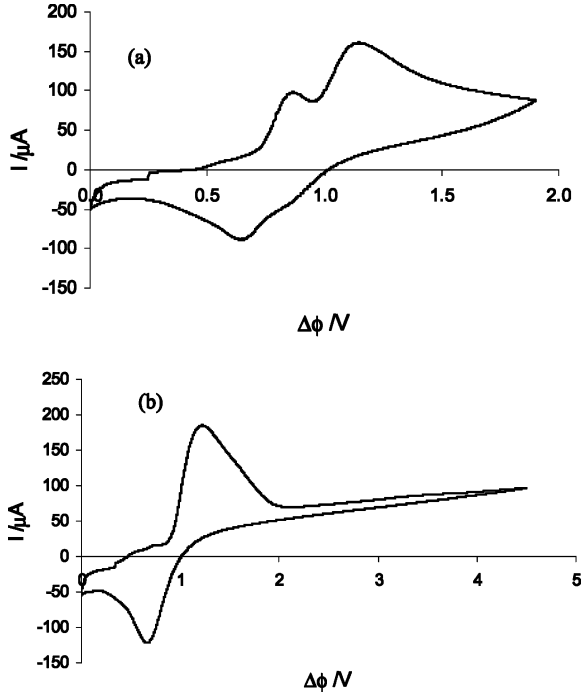

Figure 7. The cyclic voltammetric data for H^+ in the presence of silicalite membrane, (a) examining the right-hand side of the potential window and (b) examining a range extending well beyond the conventional potential limits. In both cases, cell 5 was employed with a voltage scan rate of 0.1 V s^{-1}.

the double peak was only observed for the first three or four scans, and gradually overlapped to produce one peak, as seen in Figure 7b. We attribute this to build up of proton concentration at the interface, after a number of sweeps, which hides the double peak feature. Figure 7b shows that a steady-state current is achieved for excursions of potential difference to values well beyond the conventional positive limits. This again could be utilized to examine the transfer of very hydrophilic ions from the aqueous phase or very hydrophobic ions from the organic phase, although the size limits would make the former case more likely. A recent report has described an alternative approach to such measurements, using ion transfer between aqueous electrolytes and a pure organic phase to extend the potential window.[55]

If we assume that the pulse at the positive potential limit is due to ion transfer from within the first layer of silicalite crystallites, it should be possible to estimate the concentration of ions within the silicalite pores and, from this, a very approximate diffusion coefficient of the ions within the pores.

The extent of charge transfer can be measured by integrating the positive potential pulse (this was found to be approximately independent of scan rate, consistent with the depletion argument from the first crystallite layer). The average charge transferred, Q_{ave}, can be converted to the number of moles of ions transferred, n_i, by Faraday's law, where z_i is the ion charge and F is Faraday's constant.

$$n_i = \frac{Q_{ave}}{z_i F} \tag{5}$$

The volume of the first layer of silicalite crystallites in the membrane, V_Z, can be simply calculated by

$$V_Z = A_Z \times d_Z \tag{6}$$

where A_Z is the area of the working face and d_Z is the average

TABLE 2: The Average Charge Transfer Measured for Various Ions, and the Corresponding Ion Concentrations within the Silicalite Membrane

ion	$10^4 Q_{ave}$/C	c_i/M	c_{bulk}/M	cell no.
Na^+	0.5	0.081	0.1	4
TMA^+	0.29	0.047	0.05	2
Li^+	0.17	0.028	0.1	4
Mg^{2+}	0.17	0.028	0.02	1
H^+	0.16	0.026	0.01	5
SO_4^{2-}	0.15	0.024	0.02	1
Cl^-	0.10	0.016	0.1 (LiCl)	4

crystallite width. The crystallite layer volume can be converted into a pore volume, V_{pore}, by multiplying by the void fraction, V_F, which has been reported for most zeolites.

$$V_{pore} = V_Z \times V_F \tag{7}$$

Therefore the concentration of the ions within the silicalite pores, $c_{i(z)}$, is

$$c_{i(z)} = \frac{n_i}{V_{pore}} \tag{8}$$

Combining eq 8 with eqs 5−7 gives

$$c_{i(z)} = \frac{Q_{ave}}{z_i F A_Z d_Z V_F} \tag{9}$$

For these experiments A_z and d_z were 0.38 cm^2 and 1.2×10^{-5} m (measured from previously reported scanning electron microscopy images of these membranes),[14] respectively, and for silicalite $V_F = 0.14$.[56] The results for these calculations are shown in Table 2.

Table 2 shows that the calculated concentrations of the ions within the silicalite pores are generally less than, or approximately equal to, the corresponding bulk solution concentrations. This is reasonable because of volume exclusion effects within the silicalite framework, where ions are sterically hindered and electrostatically repelled, so a lower concentration is maintained. Sodium ions were found to have the largest concentration within the pores; this is consistent with their smaller hydrated diameter (compared to Li^+ and Mg^{2+}). Li^+, Mg^{2+}, and H^+ were found to have similar concentrations, which would indicate that they have similar hydrated sizes, except each has a different ratio of counterions, which affects both steric and electrostatic properties. Surprisingly, it was found that in most cases there was a lower concentration of anions than cations, except for $MgSO_4$. This may be due to the strong interaction of the cations with the oxygen atoms of the silicalite framework. It was found that the calculated concentration of H^+ within the pores is higher than the bulk concentration; this may be due to the highly approximate nature of the calculation, or due to the higher diffusivities of H^+ within the silicalite membrane, meaning that ions from beyond the first layer are included. Further improvement in the calculation will be made by investigating the effect of changing the bulk concentration of various ions.

The concentration of both magnesium and sulfate ions was also found to exceed the bulk values; however, the approximate nature of this calculation precludes further analysis. Presently we are conducting experiments at the silicalite modified interface and systematically varying the aqueous electrolyte, in an attempt to gain a better understanding of the volume exclusion effect of the membrane and to develop a more accurate model for calculating the concentration of ions within the silicalite membrane. Once an accurate measurement of ion concentrations within the silicalite has been achieved, it should be possible to measure ionic diffusion coefficients within the silicalite pores.

Conclusion

The ready extension of the polarization window at the liquid/liquid interface can be achieved by modifying the interface with zeolite membranes. Use of the silicalite membrane, reported here, leads to the size exclusion of the ions employed as organic electrolyte. This approach can be used to allow the measurement of transfer potentials for extremely hydrophilic ions. The electrified liquid/liquid interface is described as a way to probe ion concentrations within zeolite frameworks. Numerous studies of zeolite modification of (solid) electrode surfaces have been reported previously:[8,9,12,13,29] but the liquid/liquid interface has the advantage that contact between the liquid phase and the silicalite is more readily achieved than with solid surfaces. The modification of this interface with silicalite imparts it with size selective and volume exclusion properties. It is hoped to extend this study to investigate the diffusion of ions within the zeolite pores with electrochemical methods, and to apply these properties to size selective sensors.

Acknowledgment. We thank the U.K. EPSRC (GR/S11596/01) for financial support.

Supporting Information Available: Plot of the peak potential dependence on peak current for the experimental system of Figure 2 and plot showing the comparison of the facilitated proton transfer data in the presence of the silicalite membrane with the simulations for a reversible charge transfer and a quasireversible electron transfer. This material is available free of charge via the Internet at http://pubs.acs.org.

References and Notes

(1) Csicsery, S. M. *Zeolites* **1984**, *4*, 202.
(2) Dwyer, J.; Rawlence, D. J. *Catal. Today* **1993**, *18*, 487.
(3) Chiang, A. S. T.; Chao, K.-J. *J. Phys. Chem. Solids* **2001**, *62*, 1899.
(4) Wang, J.; Martinez, T. *Anal. Chim. Acta* **1988**, *207*, 95.
(5) Wang, J. *Electoanalysis* **1991**, *3*, 255.
(6) Townsend, R. P.; Coker, E. N. *Stud. Surf. Sci. Catal.* **2001**, *137*, 467.
(7) Ghosh, P. K.; Bard, A. J. *J. Am. Chem. Soc.* **1983**, *105*, 5691.
(8) Doménech, A.; Doménech-Carbo, M. T.; Garcia, H.; Gallatero, M. S. *Chem. Commun.* **1999**, 2173.
(9) Zhang, Y.; Chen, F.; Zhang, J.; Tang, Y.; Wang, D.; Wang, Y.; Dong, A.; Ren, N. *Chem. Commun.* **2002**, 2814.
(10) Bélanger, S.; Hupp, J. T.; Stern, C. L.; Slone, R. V.; Watson, D. F.; Carrell, T. G. *J. Am. Chem. Soc.* **1999**, *121*, 557.
(11) Jirage, K. B.; Hulteen, J. C.; Martin, C. R. *Science* **1997**, *278*, 655.
(12) Rolison, D. R. *Chem. Rev.* **1990**, *90*, 867.
(13) Walcarius, A. *Electroanalysis* **1996**, *8*, 971.
(14) Dryfe, R. A. W.; Holmes, S. M. *J. Electroanal. Chem.* **2000**, *483*, 144.
(15) Lillie, G. C.; Dryfe, R. A. W.; Holmes, S. M. *Analyst* **2001**, *126*, 1857.
(16) Vanýsek, P. *Electrochim. Acta* **1995**, *40*, 2841.
(17) Reymond, F.; Fermin, D.; Lee, H. J.; Girault, H. H. *Electrochim. Acta* **2000**, *45*, 2647.
(18) Senda, M.; Kakiuchi, T.; Osakai, T. *Electrochim. Acta* **1991**, *36*, 253.
(19) Lee, H. J.; Girault, H. H. *Anal. Chem.* **1998**, *70*, 4280.
(20) Stephenson, M. J.; Holmes, S. M.; Dryfe, R. A. W. *Angew. Chem., Int. Ed.* **2005**, *44*, 3075.
(21) Ulmeanu, S. M.; Jensen, H.; Samec, Z.; Bouchard, G.; Carrupt, P.-A.; Girault, H. H. *J. Electroanal. Chem.* **2002**, *530*, 10.
(22) Ruthven, D. M.; Post, M. F. M. *Stud. Surf. Sci. Catal.* **2001**, *137*, 525.
(23) Jobic, H.; Bee, M.; Kearley, G. J. *Zeolites* **1989**, *9*, 312.
(24) Kärger, J. *Z. Phys. Chem.* (*Leipzig*) **1971**, *248*, 27.
(25) Eic, M.; Ruthven, D. M. *Zeolites* **1988**, *8*, 40.

(26) Haag, W. O.; Lago, R. M.; Weisz P. B. *Faraday Discuss*. **1981**, *72*, 312.
(27) Awum, F.; Narayan, S.; Ruthven, D. M. *Ind. Eng. Chem. Res*. **1988**, *27*, 1510.
(28) Ruthven, D. M.; Stapleton, P. *Chem. Eng. Sci*. **1993**, *58*, 89.
(29) Baker, M. D.; McBrien, M.; Burgess, I. *J. Phys. Chem. B* **1998**, *102*, 2905.
(30) Auerbach, S. *Int. Rev. Phys. Chem.* **2000**, *19* (No. 2), 155.
(31) Baerlocher, Ch.; Meier, W. M.; Olson, D. H. *Atlas of zeolite framework types*, 5th ed.; Elsevier: London, UK, 2001; p 184.
(32) Kiyozumi, Y.; Mizukami, F.; Maeda, K.; Kodzasa, T.; Toba, M.; Niwa, S.-I. *Stud. Surf. Sci. Catal.* **1997**, *105*, 2225.
(33) Fermín, D. J.; Duong, H. D.; Ding, Z. F.; Brevet, P. F.; Girault, H. H. *Phys. Chem. Chem. Phys*. **1999**, *1*, 1461.
(34) Clarke, D. J.; Schiffrin, D. J.; Wiles, M. C. *Electrochim. Acta* **1989**, *34*, 767.
(35) Girault, H. H.; Schriffrin, D. J. In *Electroanalytical Chemistry*; Bard, A. J., Ed.; Marcel Dekker: New York, 1989; Vol. 15, p 1.
(36) Marcus, Y. *Rev. Anal. Chem*. **1980**, *5*, 53.
(37) Kotz, J. C.; Purcell, K. F. *Chemistry and chemical reactivity*, 2nd ed.; Saunders College Publishing: London, UK, 1987; p 346.
(38) Shao, Y.; Stewart, A. A.; Girault, H. H. *J. Chem. Soc., Faraday Trans*. **1991**, *87*, 2593.
(39) King, K. *J. Phys. Chem*. **1970**, *74*, 4590.
(40) Bond, A. M.; Feldberg, S. W. *J. Phys. Chem. B* **1998**, *102*, 9966.
(41) Bond, A. M.; Coomber, D. C.; Feldberg, S. W.; Oldham, K. B.; Vu, T. *Anal. Chem.*, **2001**, *73*, 352.
(42) Bruhn, C.; Preetz, W. *Acta Crystallogr. C* **1997**, *C53*, 63.
(43) Jenkins, H. D. B.; Thakur, K. P. *J. Chem. Ed*. **1979**, *56*, 576.
(44) Shioya, T.; Nishizawa, S.; Teramae, N. *J. Am. Chem. Soc.* **1998**, *120*, 11534.
(45) Osakai, T.; Ebina, K. *J. Phys. Chem. B* **1998**, *102*, 5691.
(46) Shannon, R. D. *Acta Crystallogr*. **1976**, *A32*, 751.
(47) Yuan, Y.; Shao, Y. *J. Phys Chem. B* **2002**, *106*, 7809.
(48) Osborne, M. C.; Shao, Y.; Pereira, C. M.; Girault, H. H. *J. Electroanal. Chem*. **1994**, *364*, 155.
(49) Beattie, P. D.; Delay, A.; Girault, H. H. *J. Electroanal. Chem*. **1995**, *380*, 167.
(50) Amatore, C.; Savéant, J. M.; Tessier, D. *J. Electroanal. Chem*. **1983**, *147*, 39.
(51) Dryfe, R. A. W., D. Philos. thesis, Oxford University, 1995.
(52) Milner, D. F.; Weaver, M. J. *Anal. Chim. Acta* **1987**, *198*, 245.
(53) Stephenson, M. J.; Holmes, S. M.; Dryfe, R. A. W. *Electrochem. Commun*. **2004**, *6*, 294.
(54) Bard, A. J.; Faulkner, L. R. *Electrochemical Methods*: *Fundamentals and Applications*, 2nd ed.; Wiley: New York, 2001; p 147.
(55) Sun, P.; Laforge, F. O.; Mirkin, M. V., *J. Am. Chem. Soc.* **2005**, *127*, 8596.
(56) Ruthven, D. M. *Verified synthesis of zeolitic materials*, 2nd ed.; Elsevier: London, UK, 2001; p 61.